Academia Open
Vol 9 No 2 (2024): December
DOI: 10.21070/acopen.9.2024.9510 . Article type: (Clinical Research)

Table Of Content

ISSN 2714-7444 (online), https://acopen.umsida.ac.id, published by Universitas Muhammadiyah Sidoarjo

Academia Open
Vol 9 No 2 (2024): December
DOI: 10.21070/acopen.9.2024.9510 . Article type: (Clinical Research)

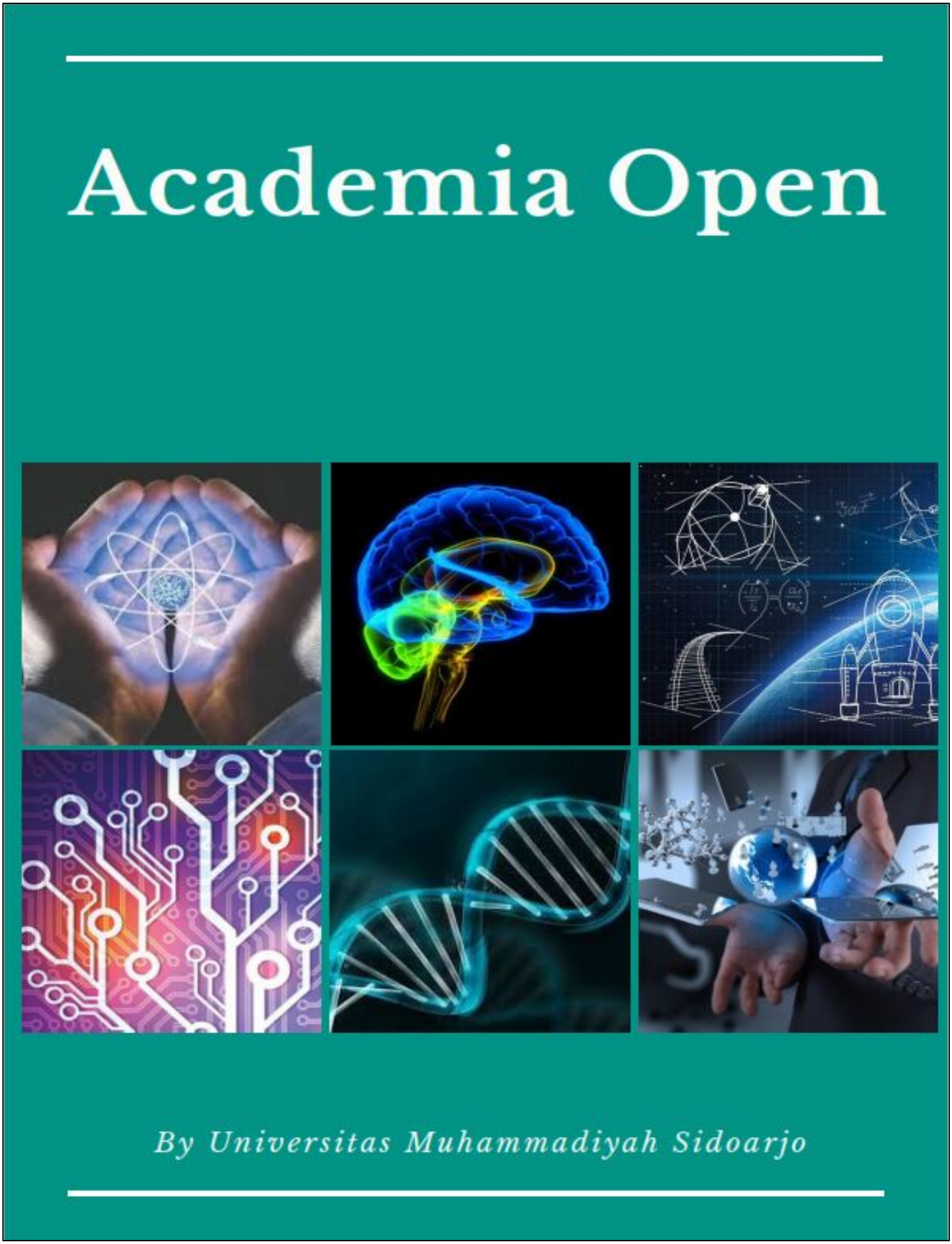

ISSN 2714-7444 (online), https://acopen.umsida.ac.id, published by Universitas Muhammadiyah Sidoarjo

Academia Open
Vol 9 No 2 (2024): December
DOI: 10.21070/acopen.9.2024.9510 . Article type: (Clinical Research)

Originality Statement

The author[s] declare that this article is their own work and to the best of their knowledge it contains no materials previously published or written by another person, or substantial proportions of material which have been accepted for the published of any other published materials, except where due acknowledgement is made in the article. Any contribution made to the research by others, with whom author[s] have work, is explicitly acknowledged in the article.

Conflict of Interest Statement

The author[s] declare that this article was conducted in the absence of any commercial or financial relationships that could be construed as a potential conflict of interest.

Copyright Statement

Academia Open
Vol 9 No 2 (2024): December
DOI: 10.21070/acopen.9.2024.9510 . Article type: (Clinical Research)

EDITORIAL TEAM

ISSN 2714-7444 (online), https://acopen.umsida.ac.id, published by Universitas Muhammadiyah Sidoarjo

Academia Open
Vol 9 No 2 (2024): December
DOI: 10.21070/acopen.9.2024.9510 . Article type: (Clinical Research)

Article information

Check this article update (crossmark)

Check this article impact (*)

Save this article to Mendeley

(*) Time for indexing process is various, depends on indexing database platform

ISSN 2714-7444 (online), https://acopen.umsida.ac.id, published by Universitas Muhammadiyah Sidoarjo

Academia Open
Vol 9 No 2 (2024): December
DOI: 10.21070/acopen.9.2024.9510 . Article type: (Clinical Research)

Investigation and Finite Element Analysis of The Distal Weight-Bearing Implant

Investigasi dan Analisis Elemen Hingga dari Implan Penahan Berat Distal

Muntadher Saleh Mahdi, st.muntadher.s.mahdi.msc@ced.nahrainuniv.edu.iq, (1)
Department of Prosthetics & Orthotics Engineering, College of Engineering, Al-Nahrain University, Baghdad, Iraq, Iraq

Dunya Abdulsahib Hamdi, dunia.abdalsahip@nahrainuniv.edu.iq, (0)
2) Department of Prosthetics & Orthotics Engineering, College of Engineering, Al-Nahrain University, Baghdad, Iraq, Iraq

(1) Corresponding author

Abstract

General Background: Osseointegration. a critical advancement in prosthetics, significantly benefits individuals with transfemoral amputations by enhancing their quality of life through innovative implant systems. **Specific Background:** The study examines a novel distal weight-bearing implant from 17 global systems, featuring a composite nanocoating of hydroxyapatite and silica, evaluated through finite element analysis and mechanical testing. **Knowledge Gap:** Research on nanocoating's impact on mechanical performance and its integration into advanced prosthetic designs is limited, despite extensive exploration of various implant systems. **Aims:** The study evaluates the distal weight-bearing implant's effectiveness, focusing on the nanocoating's role in shock absorption and mechanical stability during various gait cycle phases. **Results:** The design process involved creating a Ti-6Al-4V femoral stem and UHMWPE spacer, with the implant subjected to FEA under gait cycle conditions. Nanocoated samples demonstrated effective shock absorption, though with slightly reduced mechanical properties. The implant's performance was evaluated for heel strike, midstance, and pre-swing phases, showing adequate load-bearing capacity within safe thresholds. **Novelty:** This study introduces a detailed analysis of nanocoating impacts on implant performance and integrates biomechanical forces into FEA for enhanced prosthetic design evaluation. **Implications:** Research indicates nanocoating enhances shock absorption, but further studies are needed to balance mechanical properties with biocompatibility and biological response, potentially improving amputee care outcomes.

Highlights:

1. Advanced Implant Design: Transition from transfemoral to knee disarticulation.
2. Nanocoating Impact: Enhances shock absorption; minor mechanical property reduction.
3. FEA Results: Confirms load-bearing capacity through gait cycle phases.

Keywords: osseointegration, distal weight-bearing implant, nanocoating, finite element analysis, gait cycle

ISSN 2714-7444 (online), https://acopen.umsida.ac.id, published by Universitas Muhammadiyah Sidoarjo

Academia Open
Vol 9 No 2 (2024): December
DOI: 10.21070/acopen.9.2024.9510 . Article type: (Clinical Research)

Published date: 2024-08-12 00:00:00

Academia Open
Vol 9 No 2 (2024): December
DOI: 10.21070/acopen.9.2024.9510 . Article type: (Clinical Research)

Introduction

The Osseo-integrated prostheses for the rehabilitation of amputees (OPRA) treatment protocol was instituted in 1999 [1]. The intermediate-term success of OPRA design implants sparked interest in developing bone-anchored amputation prostheses on a global scale. Putting together the best parts of a conventional socket and an Osseo-integrated prosthesis has created a new and developing idea: a design that combines the two. The observation that patients with knee disarticulation amputation maintain their independent living status more effectively than those with transfemoral amputation (TFA) inspired the development of the distal weight-bearing implant [2]. The distal weight-bearing implant is shown in Figure 1.

Figure 1. *The distal weight-bearing implant, that comprise of four components: stem, spacer (artificial condyle), plug, and screw [3, 4].*

Following an extensive review and analysis of over thirty studies pertaining to medical implants, the distal weight-bearing implant was selected for investigation and development. The idea of the distal weight-bearing implant was that people with knee disarticulation amputation benefit from having distal support inside the traditional socket and having their weight directly transferred to their remaining limbs when the femoral condyles are kept, which is not the case with TFA as shown in Figure 2. Patients with this implant can also choose between traditional sockets or prostheses attached to their bones with this implant type as shown in Figure 3 [3].

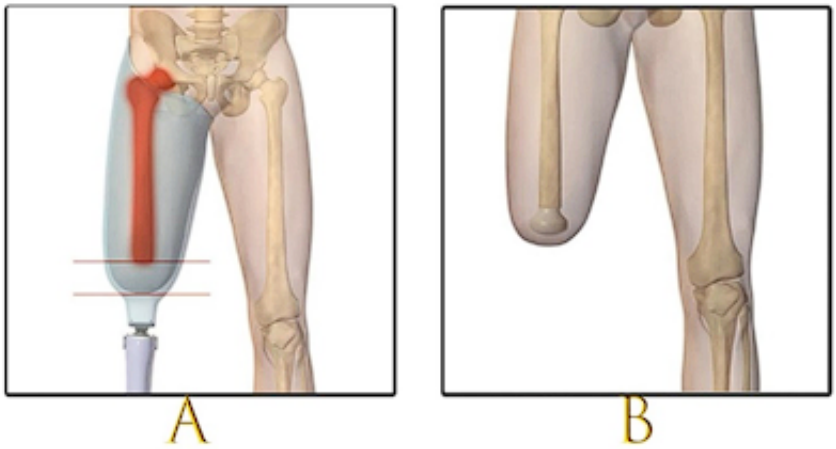

Figure 2. *A three-dimensional model of TFA both with and without the distal weight-bearing implant, as (A) amputation without implant while (B) shows the remaining limb with the implant that kept the femoral condyle.*

ISSN 2714-7444 (online), https://acopen.umsida.ac.id, published by Universitas Muhammadiyah Sidoarjo

Academia Open
Vol 9 No 2 (2024): December
DOI: 10.21070/acopen.9.2024.9510 . Article type: (Clinical Research)

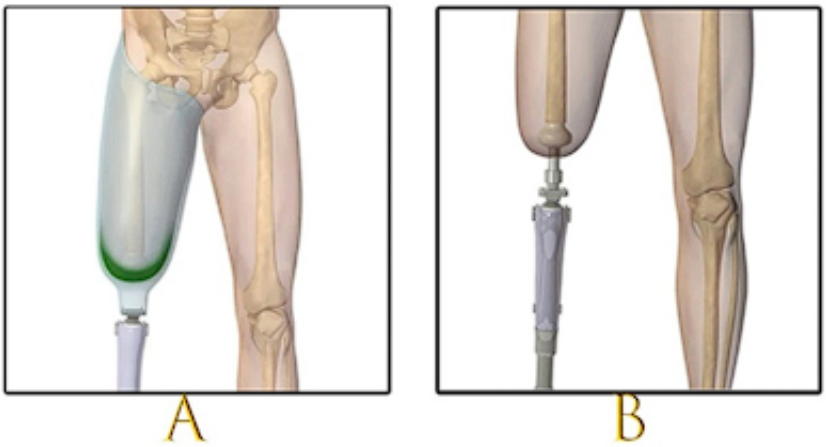

Figure 3. *A three-dimensional model of transfemoral amputee with a distal weight-bearing implant who can choose between (A) a traditional socket or (B) prostheses attached to his bone.*

As the optimal materials for Osseo-integrated prosthetic applications have yet to be identified, ongoing investigations and experiments have been conducted to attain this objective. Continuous improvement of the material selection for the implants or coating layers is imperative to achieving the intended purpose. The lifespan of the implants surpassing that of the patient would be optimal. Titanium implant materials have become increasingly important due to increased life expectancy and the demands on people's quality of life [5]. The Ti-6Al-4V alloy has excellent mechanical strength and is the most popular titanium alloy [6].

Coating titanium implants with bioactive and biocompatible materials improves their surface and eliminates the corrosion issue [7]. Because of their high bioactivity, biocompatibility, and corrosion resistance, bio-ceramics are a great substitute for load-bearing uses [8]. Hydroxyapatite is the principal mineral constituent found in human bones and teeth; it is a bio-ceramic that exhibits promise as a bone replacement material due to its non-inflammatory nature during body interactions [9, 10]. It can enhance Hydroxyapatite’s bioactivity, even if its biocompatibility is superb.

Nanotechnology entails the investigation and technological advancement of materials, devices, and systems within the size range of 0.1–100 nm, with the primary objective of producing goods that are more durable, affordable, and accurate [11]. Nanotechnology aims to improve the efficacy of implants by modifying their surface topography to increase biocompatibility, altering their composition to enhance mechanical properties, and influencing tissue responses to accelerate healing and enable immediate loading by modulating bone formation [11].

Methods

1. Design of The Distal Weight-Bearing Implant

Conducting dimensions and measurements and identifying the material composition were the initial steps in the design process; this was done through the references [3, 12]. Subsequently, the implant was meticulously crafted using the SOLIDWORKS software.

The femoral stem was composed of a Ti-6Al-4V alloy, which allowed for secure placement into the remaining femoral canal. The femoral stem has a length that varies between 120 and 180 mm, with a diameter ranging from 11 to 17 mm. These measurements depend on the length of the amputated end and the diameter of the bone. The second component consisted of a spacer (synthetic condyle) composed of UHMWPE with a diameter ranging from 54 to 62 mm. The spacer was attached to the stem by the last components, which were a Ti-6Al-4V screw and a UHMWPE plug. The spacer or cushion facilitated the distal support of the residuum within the socket, as shown in Figure 3A. Finally, the medical implant was assembled and implanted inside the femur model to be ready for FEA.

2. Nanocoating Process and Mechanical Testing

Specimens for hardness and compression tests were manufactured with precise dimensions and for specific conditions in accordance with established references [13, 14]. Each of them underwent a surface modification stage. The surface modification stage involves a series of procedures, including polishing and cleaning. The final step is the nanocoating being applied to the specimens. Six samples of Ti-6Al-4V alloy were coated with a nanomaterial consisting of 10% silica and 90% hydroxyapatite using a plasma cold spray process. Three of these samples were used for hardness testing, while the remaining were used for compression testing. The other six samples were uncoated. By comparing the mechanical parameters of the nanocoated and uncoated samples, it can

ISSN 2714-7444 (online), https://acopen.umsida.ac.id, published by Universitas Muhammadiyah Sidoarjo

Academia Open
Vol 9 No 2 (2024): December
DOI: 10.21070/acopen.9.2024.9510 . Article type: (Clinical Research)

determine whether the coating would be a beneficial addition to the distal weight-bearing implant.

3. FEA for The Implant at Gait Cycle

A static structural analysis system was implemented in ANSYS. The material types, Ti-6Al-4V and nanocoated Ti-6Al-4V, obtained from mechanical tests, have been input into the ANSYS software database. The reference materials used are the femur and UHMWPE [15, 16]. Then, the distal weight-bearing implants are divided into tiny tetrahedral samples via interlocking. In the case of static structural, the element quality is utilized, and the tetrahedral element has a dimension of 5.0 mm. In the implant are the nodes (45,710) and elements (25,200).

The implant was subjected to boundary conditions during three specific periods of the gait cycle: the heel strike phase, the midstance phase, and the pre-swing phase. These stages are crucial and serve as transitions in the gait cycle, demonstrating the degree of mechanical effectiveness of the implant.

In order to prevent the contact elements from moving past each other, the implant-bone connection was set to be fully bonded. A weight estimate of 85 kg was made for the amputee. The hip joint is capable of transferring significant loads, up to seven or eight times one's body weight during the midstance moment [17]. Based on the reference, it may be estimated that the force acting on the implant head ranges from 2000 N to 4000 N; these values correspond to the assumptions made for a human weighing 50 to 100 kg [18].

The heel strike phase entails a sudden impact force as the foot makes contact with the ground. Examining the implant's reaction at this phase guarantees its ability to withstand applied loads. The pre-swing phase entails the transfer of weight from the stance limb to the swing limb. Examining the mechanical behavior during this transition is essential for the overall functioning of the implant. By utilizing a biomechanical reference to determine the loads for each of these phases, as depicted in Figure 4, it became necessary to identify the forces impacting the implant using mathematical relationships [19]. In order to determine the horizontal frictional force, it is necessary to utilize the following equation (1):

$$F_{frict} = \mu F_n \quad \text{-----(1)}$$

Figure 4.

where () is the CoF and () is the normal force and is considered the reaction force [20]. Standard organizations and individual authors have commonly recommended a COF of 0.5 on a level walking surface [21].

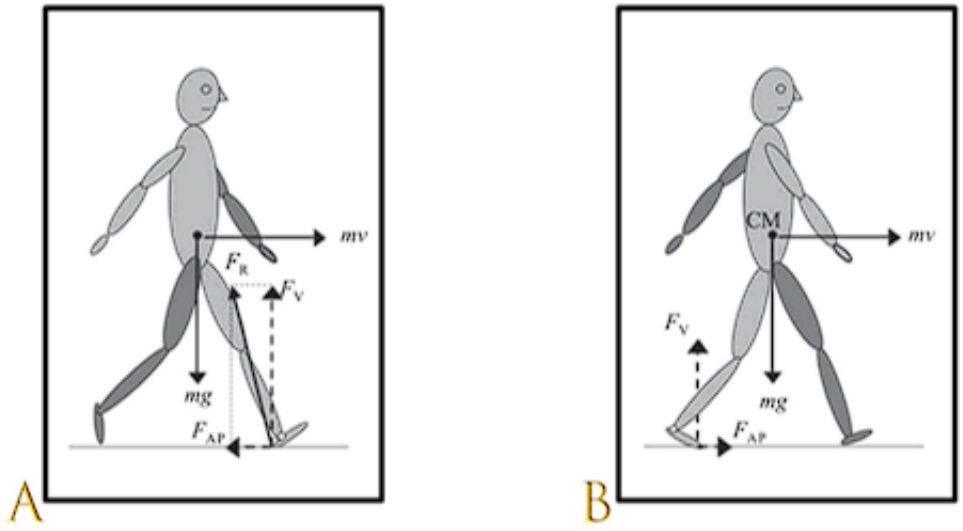

Figure 5. *The biomechanical loads that act on (A) the left foot at the heel strike phase and (B) the left foot at the pre-swing phase [19].*

In order to determine the moment generated by the reaction force at the knee joint and suppose that it is equal to the moment at the implant spacer, it needed to utilize the following equations:

Academia Open
Vol 9 No 2 (2024): December
DOI: 10.21070/acopen.9.2024.9510 . Article type: (Clinical Research)

$$M_{Knee} = M_{shank} + M_{foot} \quad \text{-----(2)}$$

where (M_{shank}) and (M_{foot}) are the moment at the lower leg and foot and they derived from the subsequent equations:

$$M_{shank} = W_{shank} \times L_{shank} \times C.G._{shank} \quad \text{-----(3)}$$

$$M_{foot} = W_{foot} \times L_{foot} \times C.G._{foot} + L_{shank} \quad \text{-----(4)}$$

where (W) and (L) are the weight and length of the body segment sequentially and ($C.G.$) is the distance from the center of gravity of the segment to the proximal endpoint [22].

Figure 6.

The vertical component of the ground reaction force is typically 2.5 to 3 times the weight of the body at the heel strike phase [23]. At the moment when the heel makes contact with the ground, the angle between the thigh bone and the body's center of gravity is roughly 30° of hip flexion [24]. This bending of the joint enables a seamless transfer of weight and provides stability when the foot first makes contact with the ground. The force of friction with the moment was derived from previous equations that considered the weight and length of the amputee and then applied to the implant spacer. During the pre-swing phase of gait, the correlation between the weight of the body and the ground reaction force acting on the femur changes. When the foot lifts off the ground, the ground reaction force acting on the femur assists in propelling the body forward. The ground reaction force during pre-swing was examined, and it was around 105.9% of an individual's body weight [25]. The angle formed between the femur and the body's center of gravity is about 10° of hip hyperextension during the pre-swing phase [24].

Result and Discussion

1. Mechanical Properties

The load was applied to the nanocoated and uncoated specimens to study the mechanical properties of the surface via the Vickers micro-hardness (HV) test. According to Table 1, in contrast with the nanocoated Ti-6Al-4V alloy (1375.9 MPa), the uncoated Ti-6Al-4V alloy exhibited an exceptionally high Vickers hardness mean (3397.1 MPa). The tensile yield stress values were also obtained. Reduce the value of Vickers micro-hardness for the nanocoated material belonging to a coated layer, which acts as a sponge that absorbs shock during implant movement and reduces pressure between the bone and the implant.

The mechanical compression test findings demonstrate a reduction in the mechanical characteristics of the Ti-6Al-4V alloy following the application of a nanocoating. Figure 5 displays the mean stress-strain curves for the coated and uncoated specimens acquired from the compression test. The findings are apparent from Table 2. The average elastic modulus reduced from (86.454 GPa) for the uncoated samples to (69.833 GPa) for the coated samples. These findings indicate that the material with the coating is more flexible than the material without the coating [26]. This could be advantageous in medical implant applications that require a certain level of flexibility, as the coating can serve as a sacrificial layer. It is worth mentioning that although the mechanical qualities have diminished, the nanocoated material may have additional benefits, such as closely resembling the properties of the bone.

The appropriateness of the coated material for utilization in medical implants would be contingent upon the particular demands of the application. It is imperative to achieve a harmonious equilibrium between the mechanical qualities of the implant material and other crucial aspects, including biocompatibility, corrosion resistance, and biological response [27]. An optimal material would achieve a harmonious equilibrium among these elements, resulting in the highest overall performance for the medical implant application. Hence, additional research and experimentation would be necessary to comprehensively assess and enhance the performance of the material.

Specimens	F (N)	D1 (µm)	D2 (µm)	HV (MPa)	Avg. HV (MPa)	Avg. Tensile Yield Strength (MPa)
Uncoated	5	52.19	52.44	3387.54	3397.1	1132.36
		51.69	51.56	3480		
		52.71	52.93	3323.68		
Nanocoated		80.77	82.36	1391.57	1375.9	458.63
		81.63	83.38	1361.38		
		81.00	83.25	1374.68		

Table 1. *The Vickers micro-hardness findings for the uncoated and nanocoated samples*

ISSN 2714-7444 (online), https://acopen.umsida.ac.id, published by Universitas Muhammadiyah Sidoarjo

Academia Open
Vol 9 No 2 (2024): December
DOI: 10.21070/acopen.9.2024.9510 . Article type: (Clinical Research)

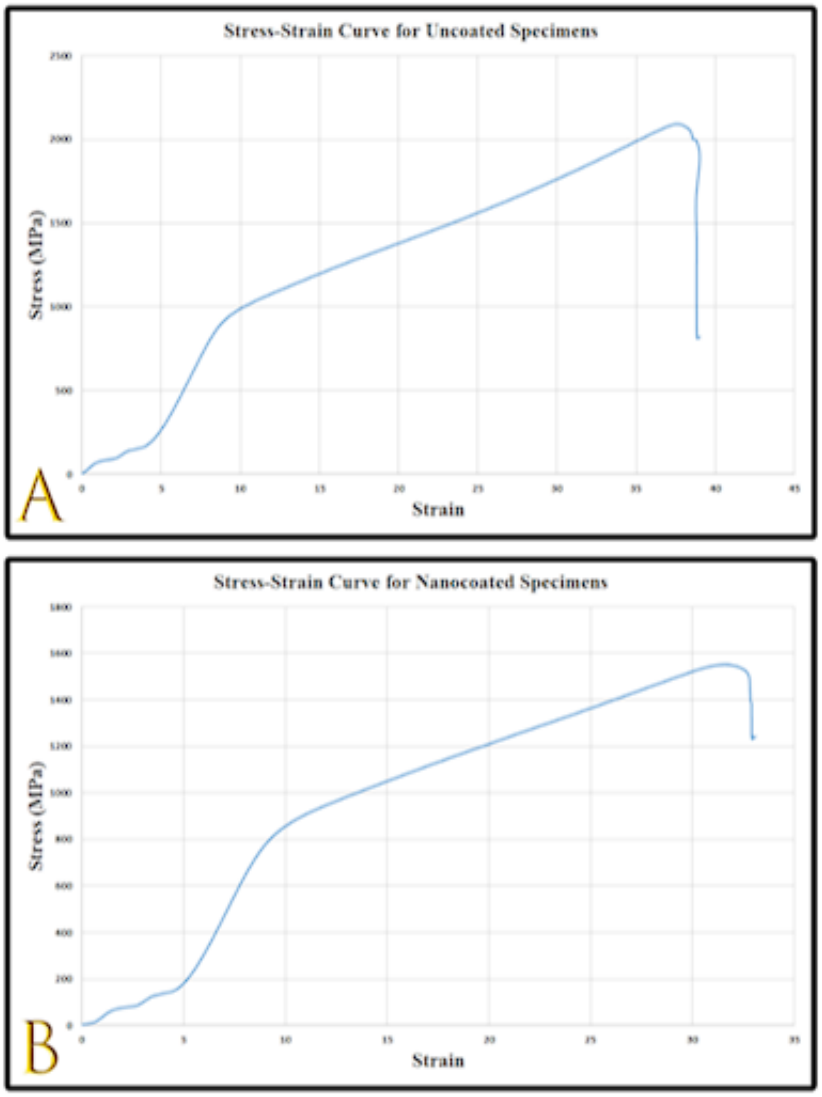

Figure 7. *The mean stress-strain curve for (A) uncoated and (B) nanocoated specimens.*

Specimens	Yield Strength (MPa)	Avg. (MPa)	Ultimate Strength (MPa)	Avg. (MPa)	Elastic Modulus (GPa)	Avg. (GPa)
Uncoated	985.1594	988.43	2078.6233	2091.27	84.222	86.454
	985.1594		2078.6233		84.222	
	994.9725		2116.5664		90.917	
Nanocoated	815.7895	855.755	1567.8671	1569.69	66.729	69.833
	905.5882		1663.2351		73.02	
	845.8864		1477.9836		69.749	

Table 2. *The mechanical properties outcomes that were derived from the stress-strain curves extracted from compression testing*

2. FEA for The Distal Weight-Bearing Implant within The Bone

With the help of the ANSYS Workbench software, the implant designs were thoroughly analyzed. The gait phases that were examined included heel strike, midstance, and pre-swing. Total deformation, Von Mises's stress, and safety factor are displayed from the lowest value (blue) to the highest value (red). In the blue area, total deformation, stress, and safety factors are minimized, while in the red area, they are maximized. The red area is often the first region to fail when the bone is subjected to high loads, as it is subjected to loads that can lead to

ISSN 2714-7444 (online), https://acopen.umsida.ac.id, published by Universitas Muhammadiyah Sidoarjo

underperformance of the design.

All the results values are summarized in Table 3. In the first case at the midstance phase, both the uncoated and nanocoated original distal weight-bearing implants experienced force application. The maximal values of Von Mises stress distribution in the bone for fully osseointegration connections, total deformation, and safety factor during the midstance phase for the uncoated and coated original implant are presented in Figure 6.

Case	Implant	Total Deformation (mm)	Von Mises Stress (MPa)	Safety Factor
Heel Strike Phase	Uncoated	0.20081	42.309	4.5317
	Nanocoated	0.21204	39.985	4.4701
Midstance Phase	Uncoated	0.14299	35.063	3.1799
	Nanocoated	0.14518	34.891	3.0869
Pre-Swing Phase	Uncoated	0.11637	34.039	5.6609
	Nanocoated	0.12891	30.849	5.0199

Table 3. *The mechanical results for the distal weight-bearing implant at the heel strike, midstance, and pre-swing phase of the gait utilizing FEA*

Based on the results obtained, it is evident that all the outcomes are safe. The highest total deformation is primarily localized in the region of the spacer, indicating that it effectively fulfills its intended function. As the spacer's material possesses ductile properties, it effectively absorbs loads and safeguards both the implant and the femur [28]. However, the comparison of the mechanical properties of the nanocoated and uncoated implants revealed that the uncoated implant exhibited slightly higher total deformation resistance and a better safety factor value. On the other hand, the coated implant demonstrated an enhancement in the Von Mises stress value. Briefly, these minor distinctions result from the brittleness of the coating components, which brings the properties of the coated implant as close as possible to those of the bone and better distributes stress by virtue of its absorption properties.

Consistent with earlier results, the present results demonstrate a distinct disparity in the mechanical characteristics of the distal weight-bearing implant during the heel strike and pre-swing phases. The results indicate that uncoated implants provide partial superiority in terms of total deformation and the value of the safety factor, similar to the results observed during the midstance phase. On the other hand, nanocoated implants offer a more suitable dispersion of stresses. Consequently, further deformation notwithstanding, it is possible to assert that the mechanical properties of the coating material have facilitated the optimal absorption and distribution of stresses while remaining within safe thresholds.

ISSN 2714-7444 (online), https://acopen.umsida.ac.id, published by Universitas Muhammadiyah Sidoarjo

Academia Open
Vol 9 No 2 (2024): December
DOI: 10.21070/acopen.9.2024.9510 . Article type: (Clinical Research)

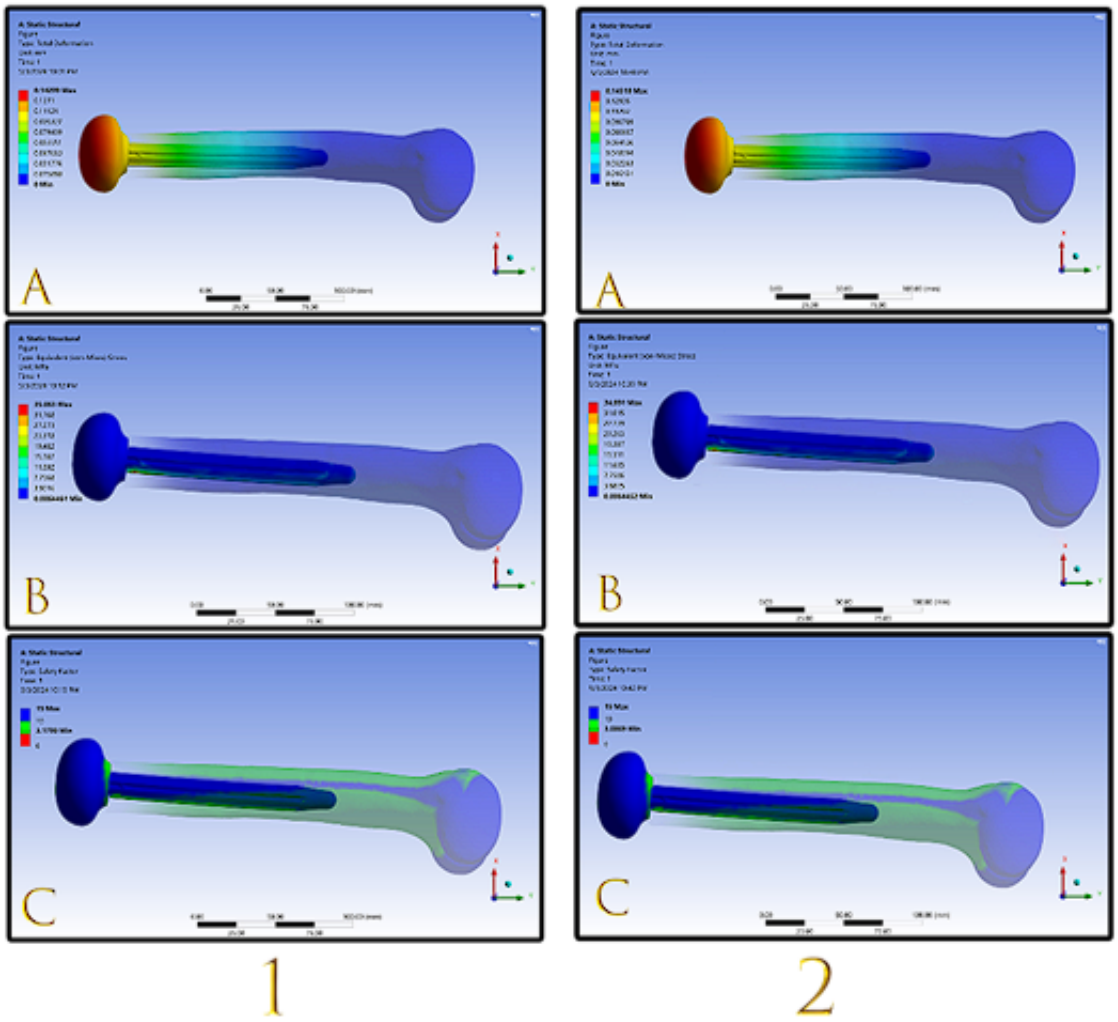

Figure 8. *The FEA results for the (1) uncoated & (2) nanocoated distal weight-bearing implant at the midstance phase include (A) the total deformation, (B) the Von Mises stress, and (C) the safety factor.*

The FEA experiments reveal the areas of total deformations, Von Mises stresses, and safety factors in both the nanocoated and uncoated distal weight-bearing implant at the heel strike and pre-swing phase, as seen in Figures 7 and 8. Typically, it is observed that the regions of deformation are confined to the spacer component, owing to the malleable characteristics that enable it to endure force-induced deformations and safeguard against damage to both the implant and the femur in which it is inserted. It is essential to mention that these results are obtained by assuming the most stringent and severe boundary conditions. Specifically, when using a traditional socket with the distal weight-bearing implant, as explained in Figure 3A, the boundary conditions will be significantly reduced, resulting in negligible risk levels. Despite these stringent boundary requirements, the results were highly secure. However, more procedures will be required to further enhance this level of safety. In terms of stress distribution, there is a drop in the area corresponding to the interface with the femur. However, this decline occurs at rates and levels that are considered safe and highly acceptable. Similarly, in terms of safety, the region with the minimum value is located at the distal end of the bone, where it connects with the femur and the implant.

The nanocoated distal weight-bearing implant exhibited the greatest degree of total deformation during the heel strike phase (0.21204 mm). This deformation surpassed that observed during other phases of gait. Despite being the highest recorded deformation number, it remains within the safe range, as indicated by the reference [29]. Furthermore, it should be mentioned that the deformation and stress values during the heel strike phase exhibit greater magnitudes. This is attributed to the motion obtained from ground reaction forces, friction, and the magnitude of the moment. However, despite these factors, it maintains a substantial safety margin and does not pose an immediate threat to the surrounding bone. In contrast, the pre-swing period is the safest since the foot in this phase is supported by the opposing foot, resulting in the most secure outcomes.

ISSN 2714-7444 (online), https://acopen.umsida.ac.id, published by Universitas Muhammadiyah Sidoarjo

Academia Open
Vol 9 No 2 (2024): December
DOI: 10.21070/acopen.9.2024.9510 . Article type: (Clinical Research)

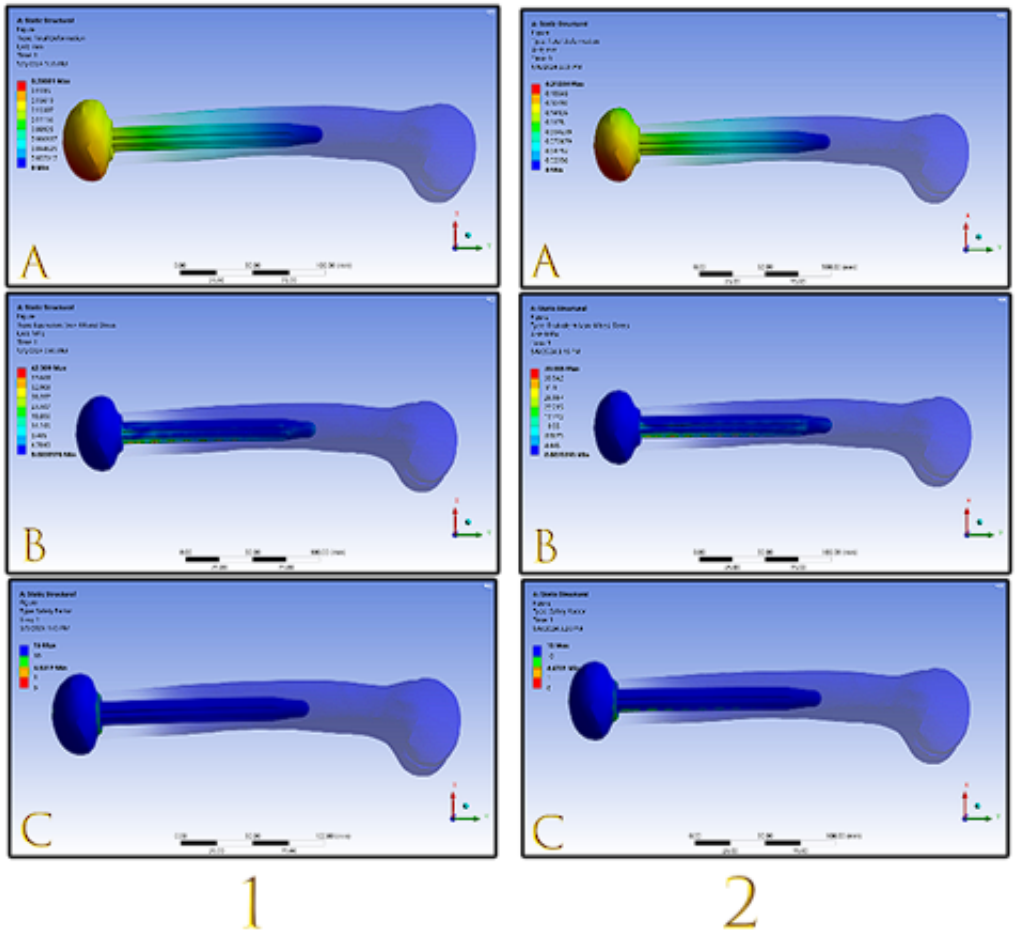

Figure 9. *The FEA results for the (1) uncoated & (2) nanocoated distal weight-bearing implant at the heel strike phase include (A) the total deformation, (B) the Von Mises stress, and (C) the safety factor.*

ISSN 2714-7444 (online), https://acopen.umsida.ac.id, published by Universitas Muhammadiyah Sidoarjo

Academia Open
Vol 9 No 2 (2024): December
DOI: 10.21070/acopen.9.2024.9510 . Article type: (Clinical Research)

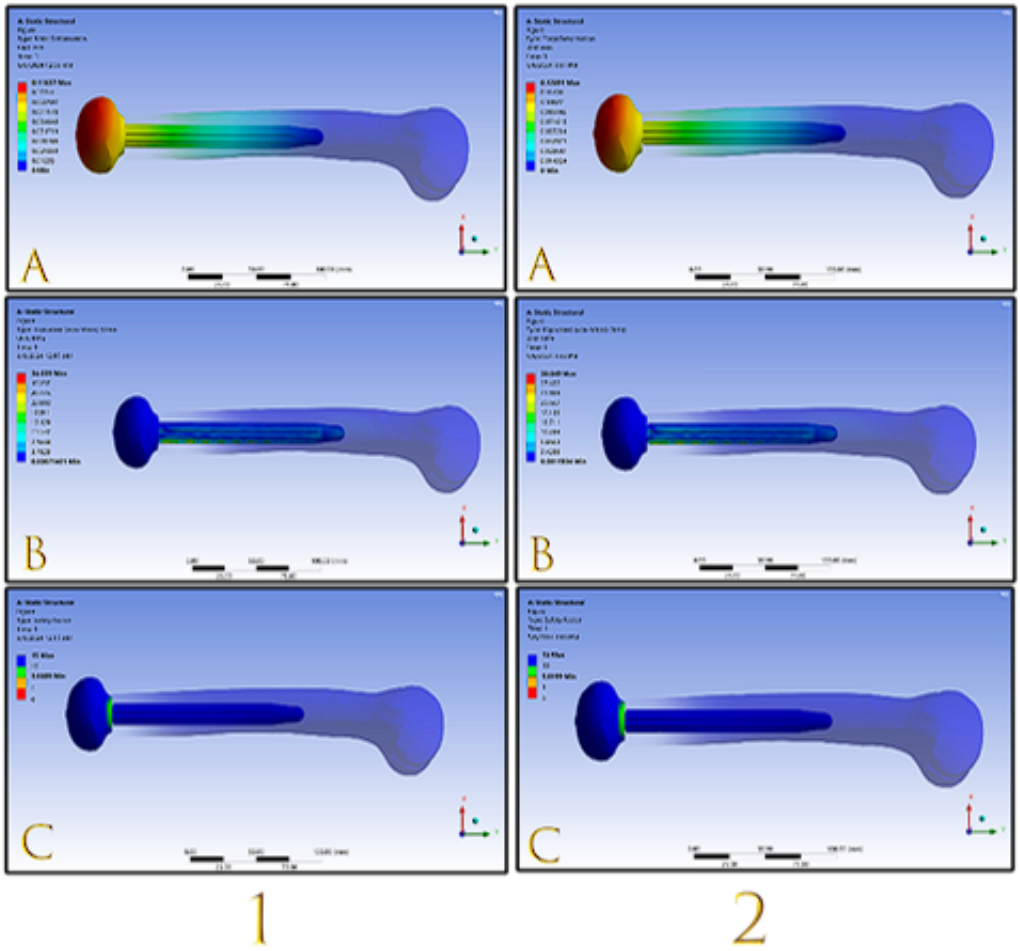

Figure 10. *The FEA results for the (1) uncoated & (2) nanocoated distal weight-bearing implant at the pre-swing phase include (A) the total deformation, (B) the Von Mises stress, and (C) the safety factor.*

Conclusion

Further deformation notwithstanding via FEA, it is possible to assert that the mechanical properties of the coating material have facilitated the optimal absorption and distribution of stresses while remaining within safe thresholds. Attaining a balanced and harmonic state between the mechanical properties of the implant material and other important factors such as biocompatibility, corrosion resistance, and biological response is of utmost importance. An ideal material would attain a balanced equilibrium among these aspects. Therefore, further investigation and testing would be required to thoroughly evaluate and improve the material's performance.

References

1. . G. A. Bertos and E. G. Papadopoulos, "Lower-Limb Prosthetics," in Handbook of Biomechatronics, Academic Press, London, 2018, pp. 241-256.
2. . T. Murakami and K. Murray, "Outcomes of Knee Disarticulation and the Influence of Surgical Techniques in Dysvascular Patients: A Systematic Review," Prosthetics and Orthotics International, vol. 40, no. 4, pp. 423-435, 2016, doi: 10.1177/0309364615574163.
3. . L. Guirao et al., "Distance and Speed of Walking in Individuals with Transfemoral Amputation Fitted with a Distal Weight-Bearing Implant," Orthopaedics & Traumatology: Surgery & Research, vol. 104, no. 6, pp. 929-933, 2018, doi: 10.1016/j.otsr.2018.04.011.
4. . L. Guirao, B. Samitier, and L. Frossard, "A Preliminary Cost-Utility Analysis of Prosthetic Care Innovations: Case of the Keep Walking Implant," Canadian Prosthetics and Orthotics Journal (CPOJ), vol. 4, no. 2, p. 11, 2021, doi: 10.33137/cpoj.v4i2.36366.
5. . M. Fellah et al., "Tribological Behavior of Ti-6Al-4V and Ti-6Al-7Nb Alloys for Total Hip Prosthesis," Advances in Tribology, vol. 2014, p. 451387, 2014, doi: 10.1155/2014/451387.
6. . J. Katic, S. Krivacic, Z. Petrovic, D. Mikic, and M. Marcius, "Titanium Implant Alloy Modified by

Electrochemically Deposited Functional Bioactive Calcium Phosphate Coatings," Coatings, vol. 13, no. 3, p. 640, 2023, doi: 10.3390/coatings13030640.
7. . M. Catauro et al., "Coating of Titanium Substrates with ZrO2 and ZrO2-SiO2 Composites by Sol-Gel Synthesis for Biomedical Applications: Structural Characterization, Mechanical and Corrosive Behavior," Coatings, vol. 9, no. 3, p. 200, 2019, doi: 10.3390/coatings9030200.
8. . D. Shekhawat, A. Singh, M. Banerjee, T. Singh, and A. Patnaik, "Bioceramic Composites for Orthopaedic Applications: A Comprehensive Review of Mechanical, Biological, and Microstructural Properties," Ceramics International, vol. 47, no. 3, pp. 3013-3030, 2021, doi: 10.1016/j.ceramint.2020.09.214.
9. . J. A. Garibay-Alvarado, L. F. Espinosa Cristóbal, and S. Y. Reyes-López, "Fibrous Silica-Hydroxyapatite Composite by Electrospinning," Producto de Investigación ICB, vol. 5, no. 2, p. 1701, 2017, doi: 10.29121/granthaalayah.v5.i2.2017.1701.
10. . R. Ravarian, F. Moztarzadeh, M. S. Hashjin, S. Rabiee, P. Khoshakhlagh, and M. Tahriri, "Synthesis, Characterization and Bioactivity Investigation of Bioglass/Hydroxyapatite Composite," Ceramics International, vol. 36, no. 1, pp. 291-297, 2010, doi: 10.1016/j.ceramint.2009.09.016.
11. . S. T. Ozak and P. Ozkan, "Nanotechnology and Dentistry," European Journal of Dentistry, vol. 7, no. 1, pp. 145-151, 2013, doi: 10.1055/s-0039-1699010.
12. . L. Guirao, C. B. Samitier, M. Costea, J. M. Camos, M. Majo, and E. Pleguezuelos, "Improvement in Walking Abilities in Transfemoral Amputees with a Distal Weight Bearing Implant," Prosthetics and Orthotics International, vol. 41, no. 1, pp. 26-32, 2017, doi: 10.1177/0309364616633920.
13. . S. S. d. Rocha, G. L. Adabo, G. E. P. Henriques, and M. A. d. A. Nóbilo, "Vickers Hardness of Cast Commercially Pure Titanium and Ti-6Al-4V Alloy Submitted to Heat Treatments," Brazilian Dental Journal, vol. 17, pp. 126-129, 2006, doi: 10.1590/S0103-64402006000200008.
14. . R. Papirno, J. F. Mescall, and A. M. Hansen, "Fracture in Axial Compression Tests of Cylinders," in Compression Testing of Homogeneous Materials and Composites, ASTM International, 1983.
15. . P. Prochor and E. Sajewicz, "A Comparative Analysis of Internal Bone Remodelling Concepts in a Novel Implant for Direct Skeletal Attachment of Limb Prosthesis Evaluation: A Finite Element Analysis," Proceedings of the Institution of Mechanical Engineers, Part H: Journal of Engineering in Medicine, vol. 232, no. 3, pp. 289-298, 2018, doi: 10.1177/0954411917751003.
16. . J. B. Park and J. D. Bronzino, Biomaterials: Principles and Applications, CRC Press, 2002.
17. . L. Mattei, F. Di Puccio, B. Piccigallo, and E. Ciulli, "Lubrication and Wear Modelling of Artificial Hip Joints: A Review," Tribology International, vol. 44, no. 5, pp. 532-549, 2011, doi: 10.1016/j.triboint.2010.06.010.
18. . P. Prochor, S. Piszczatowski, and E. Sajewicz, "Biomechanical Evaluation of a Novel Limb Prosthesis Osseointegrated Fixation System Designed to Combine the Advantages of Interference-Fit and Threaded Solutions," Acta of Bioengineering and Biomechanics, vol. 18, no. 4, pp. 21-31, 2016, doi: 10.5277/ABB-00642-2016-02.
19. . A. E. Chapman, Biomechanical Analysis of Fundamental Human Movements, Human Kinetics, 2008.
20. . V. L. Popov, Contact Mechanics and Friction, Springer, 2010.
21. . T. Lockhart, "Biomechanics of Human Gait-Slip and Fall Analysis," in Encyclopedia of Forensic Sciences: Second Edition, Elsevier Inc., 2013, pp. 466-476.
22. . A. Tözeren, Human Body Dynamics: Classical Mechanics and Human Movement, Springer Science & Business Media, 1999.
23. . S. A. Meardon, "Biomechanics and Stress Fractures: Utility of Running Gait Analysis," in Stress Fractures in Athletes: Diagnosis and Management, Springer, 2020, pp. 107-128, doi: 10.1007/978-3-030-46919-1_8.
24. . S. J. Shultz, P. A. Houglum, and D. H. Perrin, Examination of Musculoskeletal Injuries, Human Kinetics, 2015.
25. . Z. M. Kokolevich, E. Biros, O. Tirosh, and J. E. Reznik, "Distinct Ground Reaction Forces in Gait Between the Paretic and Non-Paretic Leg of Stroke Patients: A Paradigm for Innovative Physiotherapy Intervention," Healthcare, vol. 9, no. 11, p. 1542, 2021, doi: 10.3390/healthcare9111542.
26. . J. Zhao, K. Liu, M. Ding, L. Yin, and S. Liang, "Relationship Between the Composition and Elastic Modulus of TiZrTa Alloys for Implant Materials," Metals, vol. 12, no. 10, p. 1582, 2022, doi: 10.3390/met12101582.
27. . Y. K. Balasubramanian Gayathri, R. L. Kumar, V. V. Ramalingam, G. S. Priyadharshini, K. S. Kumar, and T. R. Prabhu, "Additive Manufacturing of Ti-6Al-4V Alloy for Biomedical Applications," Journal of Bio-and Tribo-Corrosion, vol. 8, no. 4, p. 98, 2022, doi: 10.1007/s40735-022-00700-1.
28. . M. Hussain et al., "Ultra-High-Molecular-Weight-Polyethylene (UHMWPE) as a Promising Polymer Material for Biomedical Applications: A Concise Review," Polymers, vol. 12, no. 2, p. 323, 2020, doi: 10.3390/polym12020323.
29. . H. Göktaş et al., "Optimization of Hip Implant Designs Based on Its Mechanical Behaviour," in Biomechanics in Medicine, Sport and Biology, Springer, 2022, pp. 37-43, doi: 10.1007/978-3-030-86297-8_4.

ISSN 2714-7444 (online), https://acopen.umsida.ac.id, published by Universitas Muhammadiyah Sidoarjo